Dynamics in Adsorbed Layers of Associative Polymers in the Limit of Strong Backbone−Surface Attractions

Yaodong Huang and Maria M. Santore*,†

Department of Chemical Engineering, Lehigh University, 111 Research Drive, Bethlehem, Pennsylvania 18015

Received July 30, 2001. In Final Form: November 29, 2001

Taken together with the shape of the adsorption isotherm, the adsorption and desorption dynamics of hydrophobically end-modified poly(ethylene oxide) (PEO) on silica suggest that adsorbed layers are comprised of two general populations: a tightly adsorbed underlayer and a loosely bound outer layer. The former is driven by a large number of hydrogen bonding interactions between the PEO's ether groups and nondissociated surface silanols, per the classical model of homopolymer adsorption with tails, loops, and trains. The outer layer is held in place by hydrophobic interactions, about 7−8 kT between the chain ends. In the dilute limit, transport-limited adsorption kinetics suggests that chains adsorb individually and that the adsorbed layer contains only the chains tightly bound via backbone−surface interactions. At greater free solution concentrations, still dilute, entire clusters adsorb and the layer contains both tightly bound and hydrophobically associated populations. The loosely bound outer layer responds to flow: The steady-state adsorbed amount depends on the wall shear rate, decreasing in stronger flows. The loosely bound layer also desorbs at the transport-limited rate in flowing water, facilitating quantification of its binding strength through the application of a hybrid isotherm model combining features of a Langmuir isotherm with those predicted from mean-field treatments of homopolymer adsorption.

Introduction

Hydrophobically modified water soluble polymers comprise an interesting fundamental system, as well as additives in paints and coatings, where they act as rheological modifiers, imparting desirable flow properties without a yield stress or high elongational viscosities.[1] The class of hydrophobically modified polymers that has received the most scientific attention is telechelics, or linear chains with end-group hydrophobes. Several groups have studied different series of such molecules, where a linear poly(ethylene oxide) (PEO) chain is capped with alkane hydrophobes.[2−11] In dilute solution, these molecules self-assemble into flowerlike micelles where, for the majority of chains, both chain ends reside in the same micelle or aggregate.[2,3,12] The aggregation number has been reported between 10 and 80 hydrophobes per associated cluster, depending on the measurement technique and the particular molecular architecture.[3,5,6,13−18] Also, the critical aggregation concentration (CAC) is reported to be quite low, though only a few investigations have focused on the most dilute regime where the CAC can be quantified.[13]

As the concentration is increased, chains bridge between micelles, imparting attractions between them and ultimately leading to the formation of an associated network.[5] The intermicelle attraction induces a phase separation, as was shown most clearly for a series of samples comprised of narrow molecular weight PEO end-capped with C16 or C18 hydrophobes.[5] Also, interesting viscoelastic properties are found in this regime. Associated solutions exhibit a single relaxation time[8] which is attributed to the disengagement of single hydrophobes from associated clusters. The solutions are also shear-thinning, with an extended zero shear plateau rather than an apparent yield stress. At higher stresses, shear thickening is seen, followed by extensive shear thinning. The original approach to describing these rheological features invoked a transient network model;[19,20] however, more recently, much of the rheology has been explained in the context of attractive micelles.[21] Even with the micellar approach to understanding the rheology, disengagement of single hydrophobes from clusters is believed to dominate the relaxation behavior: mixtures containing hydrophobes of two different lengths show a bidmodal relaxation.[22]

* To whom correspondence should be addressed.

† Present address: Department of Polymer Science, University of Massachusetts, 120 Governors Drive, Amherst, MA 01003.

(1) Schaller, E.; Sperry, P. R. *Handbook of Coatings and Additives* **1992**, *2*, 105−63.

(2) Winnik, M. A.; Yekta, A. *Curr. Opin. Colloid Interface Sci.* **1997**, *2*, 424−36.

(3) Alami, E.; Almgren, M.; Brown, W.; Francois, J. *Macromolecules* **1996**, *29*, 2229−2243.

(4) Santore, M. M.; Prud'homme, R. K.; Russel W. B. *Macromolecules* **1990**, *23*, 3821−3832.

(5) Pham, Q. T.; Russel, W. B.; Thibeault, J. C.; Lau, W. *Macromolecules* **1999**, *32*, 2996−3005.

(6) Vorobyova; O.; Yekta; A.; Winnik; Lau, W. *Macromolecules* **1998**, *31*, 8998−9007.

(7) Volpert, E.; Selb, J.; Candau, F.; Green, N.; Argillier, J. F.; Audibert, A. *Langmuir* **1998**, *14*, 1870−1879.

(8) Jenkins, R. D. Ph.D. Thesis, Lehigh University, 1990.

(9) Jenkins, R. D.; Silebi, C. A.; El-Aasser, M. S. In *Polymers as Rheology Modifiers*; Schulz, D. N., Glass, J. E. Eds.; ACS Symposium Series 462; American Chemical Society: Washington D. C., 1991.

(10) Richey, B.; Kirk, A. B.; Eisenhart, E. K.; Fitzwater, S.; Hook, J. *J. Coat. Technol.* **1991**, *63*, 31−40.

(11) Francois, J.; Maitre, S.; Rawiso, M.; Sarazin, D.; Beinert, G.; Isel, F. *Colloids Surf., A* **1996**, *9*, 881−883.

(12) Argillier, J.-F.; Audibert, A.; Lecourtier, J.; Moan, M.; Rousseau, L. *Colloids Surf., A* **1996**, *113*, 247−257.

(13) Wang, Y.; Winnik, M. A. *Langmuir* **1990**, *6*, 1437−1439.

(14) Vorobyova, O.; Lau, W.; Winnik, M. A. *Langmuir* **2001**, *17*, 1357−1366.

(15) Yekta, A.; Xu, B.; Duhamel, J.; Adiwidjaja, H.; Winnik, M. A. *Macromolecules* **1995**, *28*, 956−966.

(16) MacDonald, P. M.; Uemura, Y.; Dyke, L.; Zhu, X. *Adv. Chem. Ser.* **1996**, *248*, 377−393.

(17) Maechling-Strasser, C.; Clouet, F.; Francois, J. *Polymer* **1992**, *33*, 1021−1025.

(18) Walderhaug, H.; Hansen, F. K.; Abrahmsen, S.; Persson K.; Stilbs, P. *J. Chem. Phys.* **1993**, *97*, 8336−8342.

(19) Green, M. S.; Tobolsky, A. V. *J. Chem. Phys.* **1946**, *14*, 80−92.

(20) Tanaka, F.; Edwards, S. F. *J. Non-Newtonian Fluid Mech.* **1992**, *43*, 247−309.

(21) Pham, Q. T.; Russel, W. B.; Thibeault, J. C.; Lau, W. *Macromolecules* **1999**, *32*, 5139−5146.

10.1021/la0111912 CCC: $22.00
Published on Web 02/08/2002

In paints and coatings, polymer additives adsorb to dispersed particles, contributing to their stability or causing their flocculation,[4] as well as complicating the rheology.[8,9,23] For instance, at low frequencies, diffusional modes of dispersed particles generate a power-law spectrum of relaxation times.[24] In the most concentrated situations, the dynamics within the adsorbed layers of associative polymer may also be important. The current work examines the detailed features, both structural and dynamic, of adsorbed layers of hydrophobically end modified polymers, in particular the formation and break down of interfacial networks. While such physics is important for rheological control in paints and coatings, the general scenario of interfacial network formation and breakdown is also a paradigm that appears in biological and biomedical systems, for instance, blood flow through small capillaries, where networks growing out from the epithelial glycocalylx are disrupted and reform as blood cells pass through the restricted geometry.[25]

In this work, we investigated the adsorption of hydrophobically modified PEO, focusing on the model system comprised of a 35 000 narrow molecular weight backbone, end-capped with C16 hydrophobes. This sample, called HDU (for hexadecyl urethane), has been the focus of fundamental rheological and aggregation studies in the Lau, Winnik, and Russel laboratories.[5,6,21] The chemistry of HDU is in noted contrast with that of other hydrophobically modified PEOs that contain short PEO chains, with molecular weights about 8000, linked together with isophorone diisocyanate.[8,9,13] Samples of the latter, whose chemistry is motivated by that in commercial products, tend to have polydispersities in the range 1.5−2.0. While this polydispersity has been shown to minimally affect rheology,[22] it is a major concern in adsorption studies where surface selectivity can favor adsorption of the longest or shortest chains from the bulk solution.[26,27] Such selective adsorption is known to cause a number of experimental artifacts.[28,29]

In the current work, we examine the adsorption of HDU onto planar silica, which serves as a model for many different substrates exhibiting attractions between the surface and the main polymer backbone. Hence, hydrophobe adsorption to the surface is not the main driving force for adsorption, though the hydrophobes may indeed adsorb at some coverage levels. Here, we provide evidence based on the isotherm, adsorption, and desorption dynamics that the adsorbed layer contains two main parts: an underlayer which is tightly physisorbed to the surface and a loosely bound layer which makes up much of the interfacial mass at modest bulk solution concentrations. The latter forms a shear-responsive transient network of associated clusters. This model of an extended adsorbed layer differs from previous interpretations,[8,9,23,30] albeit with different substrates, where hydrophobes were thought to dominate the polymer-surface interaction.

Experimental Section

A sample of HDU, PEO chains with a molecular weight of 35 000 and C16 alkane end caps, was generously provided by the Rohm and Haas Company. It contained the same chemistry as the HDU studied in the Russel and Winnik laboratories.[5,6] Special care was taken to ensure that all molecules, within the detectible limit, were capped with C16 hydrophobes and that there were no free hydrophobes in the sample. Details of the synthesis and characterization are provided elsewhere.[5,6] Most relevant for the current study, our HDU sample had a reported polydispersity of 1.1, which qualifies it as having a narrow molecular weight distribution.

The HDU sample was compared with unmodified narrow molecular weight standard PEO, purchased from Polymer Laboratories and used as-is. Its molecular weight was 29 600, with a polydispersity of 1.05. The molecular weight of 29 600 was the closest available (at the time of this investigation) to the 35 000 of the HDU. Both samples were sufficiently close in chain length that reasonable comparisons could be made. Where possible, we also present some previous adsorption data employing a PEO sample of 33 000 molecular weight.[31]

pH 7.2 phosphate buffer (0.008 M Na_2HPO_4 and 0.002 M KH_2PO_4 from Fisher Scientific) was employed to control the pH. This was needed for experimental reproducibility, since PEO is known to hydrogen bond to the nondissociated silanols on the silica surface, facilitating adsorption. As the silanols site density is pH-sensitive, pH control ultimately gives reproducible adsorbed amounts.

Polymer solutions were prepared fresh for each series of adsorption experiments. Samples were dissolved at least overnight but were used within three days of their preparation, eliminating the need for antioxidants and other preservatives. At the concentrations in the current study, we observed no phase separation into a concentrated micelle phase, though we kept all solution reservoirs well-stirred as a precaution during adsorption studies.

Silica surfaces were prepared in-situ inside the reflectometer cell by exposure to concentrated sulfuric acid and were rinsed with copious amounts of deionized water, as previously described.[31] During this procedure, the surface was not exposed to air to avoid contamination. The resulting surfaces of the soda-lime glass have been shown to be silica, and adsorption of PEO onto these surfaces is highly reproducible. The silica on the slide surface has been shown to be optically distinct from the soda-lime glass making up the bulk of the slide, a feature taken into account by the reflectometry calibration procedure. [31]

A near Brewster reflectometer, equipped with a steady shear flow cell was employed to monitor the adsorption dynamics and coverages of the two polymers on silica. The details of our instrument have been described previously;[31] however, we note here that we employ a 3 mW HeNe laser which enters from the substrate rather than the solution side. Weak partial internal reflections, directed onto a detector, facilitate real-time measurement of the surface excess. The adsorbed amount follows from an optical treatment where the adsorbed layer is modeled as a step-function with a finite thickness and a single refractive index, in addition to the silica surface layer on the microscope slide.[31] Attempts to model the adsorbed layer more accurately as a series of sublayers, each with its own refractive index provided no additional information. In other words, the optical reflectometry technique can accurately measure the total surface excess but cannot resolve further structural details of the adsorbed layer. In the current study, we found a thickness of 13 nm and a refractive index of 1.49 appropriate for the glass surface layer, where the bulk substrate refractive index was 1.515. For the adsorbed layer, we found optical properties similar to those of PEO: a refractive index of 1.36 for the polymer layer and a dn/dc value of 0.134 for the polymer solution.[31]

Our flow cell was a black Teflon block with a thin rectangular flow channel of dimensions 0.15 cm by 1.0 cm by 4.0 cm. A tapered inlet port region minimized the entrance effects. Liquid was pumped through the channel between the glass surface and the Teflon channel wall, facilitating adsorption on the glass under

(22) Annable, T.; Busacall, R.; Ettalaie, R.; Whittlestone, D. *J. Rheol.* **1993**, *37*, 695−726.
(23) Pham, Q. T.; Russel, W. B.; Lau, W. *J. Rheol.* **1998**, *42*, 159−176.
(24) Pham, Q. T.; Russel, W. B.; Thibeault, J. C.; Lau, W. *J. Rheol.* **1999**, *43*, 1599−1615.
(25) Pries, A. R.; Secomb, T. W.; Jacobs, H.; Sperandio, M.; Osterloh, K.; Gaehtens, P. *Am. J. Physiol.* **1997**, *273*, H2272.
(26) Santore, M. M.; Fu, Z. *Macromolecules* **1997**, *30*, 8516−8517.
(27) Dijt, J. C.; Cohen Stuart, M. A.; Fleer, G. J. *Macromolecules* **1994**, *27*, 3219−3228.
(28) Cohen-Stuart, M. A.; Scheutjens, H. M. H. M.; Fleer, G. J. *J. Polym. Sci., Polym. Phys. Ed.* **1980**, *18*, 559−573.
(29) Fu, Z.; Santore, M. M. *Macromolecules* **1998**, *31*, 7014−7022.
(30) Ou-Yang, H. D.; Gao, Z. *J. Phys. II (France)* **1991**, *1*, 1375.
(31) Fu, Z.; Santore, M. M. *Colloids Surf., A* **1998**, *135*, 63−75.

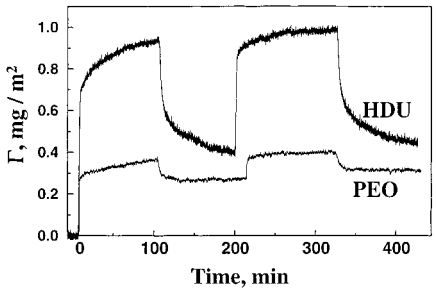

Figure 1. Adsorption and desorption kinetics for HDU and 29 K molecular weight PEO. The bulk solution concentration is 100 ppm and the wall shear rate is 8.5 s^{-1}.

shear flow conditions. The wall shear rates were calculated assuming fully developed laminar slit flow within the flow cell, which was confirmed independently.[31]

Results

Layer Structure. We start by considering the qualitative adsorption and desorption kinetics of HDU to motivate a particular interfacial structure within adsorbed layers: Figure 1 shows a pair of adsorption−desorption cycles for HDU and PEO, comparing their respective coverages in the presence of each polymer solution at a concentration of 100 ppm, and in gently flowing buffer. Initially, the cell contained flowing buffer. Then following a valve turnover, buffered polymer solution flowed through the cell and adsorption began at time zero. In the two runs, both PEO and HDU adsorbed rapidly. For PEO, the adsorption rate was nearly constant up to the saturation coverage. Beyond the rapid initial adsorption of PEO, a very slow gradual increase in coverage occurred because of polydispersity. Even narrow molecular weight standards with polydispersities of 1.05 contain significant populations of chains differing in length by a factor of 2. It has been established that during continuous flow of polymer solution over an adsorbed layer, long chains displace short ones, causing the slow sustained increase in PEO coverage in Figure 1.[26−29] In HDU, the initial adsorption rate was also fast. The approach to the final plateau involved a slow continued increase in adsorbed mass that was more pronounced than that seen with native PEO. For the HDU, the ultimate coverage was near 1 mg/m^2.

After exposing each surface to its respective polymer solution for 2 h, flowing buffer was reintroduced, continuously flushing the free polymer chains from the bulk solution and providing a driving force for desorption. In PEO, negligible desorption was observed beyond the first minute of solvent flow, in agreement with the literature.[31,32] Desorption of PEO into water or salt solutions from silica is extremely slow because the adsorption affinity is high and the shape of the adsorption isotherm provides minimal driving force for desorption, even at the transport limited rate which is the maximum possible. In Figure 1, substantial HDU desorption proceeded when buffer was pumped through the cell. Though desorption initially occurred at a moderate rate, with time it became exceedingly slow. From Figure 1, it appears that the ultimate HDU coverage would be slightly greater than that of the PEO. Indeed, we observed the HDU coverage in longer desorption runs to approach values slightly greater than that for PEO of analogous molecular weight.[33]

After 2 h of exposure to flowing buffer, the polymer solutions were reintroduced for a second adsorption cycle, followed by a second desorption cycle. This had little effect on the PEO layer where the coverage had been minimally affected by exposure to flowing water. In HDU, the coverage increased back toward its original plateau, with the adsorption kinetics of the readsorption step (beyond the transport-limited regime) faster than that of the original adsorption cycle. This suggests that the originally adsorbed HDU chains have reconfigured by the end of the first adsorption/desorption cycle, in a manner than accommodates subsequent incorporation of new chains in the second cycle. This reconfiguration may involve movement of hydrophobes away from the silica surface where they become more accessible to incoming chains or evolution of the interfacial aggregation number. Likewise, the dynamics and ultimate coverages attained for the second exposure to the buffer rinse were similar to those of the first rinse cycle.

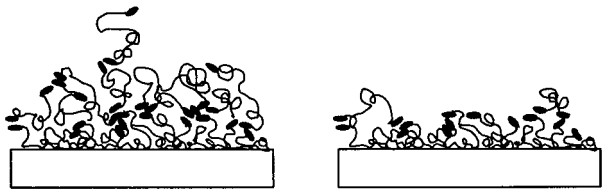

Figure 2. Schematics of adsorbed layer structures in the presence of (left) and without (right) free HDU in solution.

The adsorbed PEO layer in Figure 1 is known to be a classical homopolymer layer comprised of tails, loops, and trains.[34] Its physisorption is driven by hydrogen bonding between the polymer's ether groups and nondissociated surface silanols. This same hydrogen bonding adsorption mechanism is also available to the HDU. Indeed, Figure 1 suggests that HDU adsorption is, in part, dominated by this mechanism, as the ultimate HDU coverage in flowing buffer approaches that of unmodified PEO. (The slightly higher coverage of HDU in contact with buffer at long times may result from slight polydispersity of this sample or from residual hydrophobic associations.) If about 0.4−0.5 mg/m^2 of HDU forms, through hydrogen bonding, an "underlayer" on silica, then the additional HDU coverage can be attributed to hydrophobic associations.

Figure 2 presents a schematic illustrating possible HDU layer structures in flowing polymer and buffer solutions, respectively. The figure is meant to convey the concept that some chains are strongly bound to the surface through hydrogen bonding while others, having minimal contact with the silica, associate with the interface through hydrophobic interactions. These hydrophobically associated chains, contributing about 0.5−0.6 mg/m^2 to the adsorbed layer, have their terminal hydrophobes in contact with the hydrophobes of the underlayer of chains on the silica. Apparently, the hydrophobic associations are substantially weaker than the hydrogen bonding (on a per chain basis), so that the hydrophobically associated chains can be removed in flowing solvent while those in the underlayer are retained on the time scales of interest. In the extreme, one might identify two distinct interfacial populations, depending on whether a chain adsorbs through hydrophobic interactions or hydrogen bonding. In reality, however, we expect a smooth distribution of populations between these two extremes, with varying degrees of hydrophobic and hydrogen bonding interactions. Also, while Figure 2 shows hydrophobic clusters in the layer but not on the surface, we should emphasize that

(32) Dijt, J. C.; Fleer, G. J.; Cohen Stuart, M. A. *Macromolecules* **1992**, *25*, 5416−5423.

(33) Huang, Y. M.S. Thesis, Lehigh University, 2001.

(34) Fleer, G. J.; Cohen Stuart, M. A.; Scheutjens, J. M. H. M.; Cosgrove, T.; Vincent, B. *Polymers at Interfaces*; Chapman Hall: London, 1993; Chapter 5.

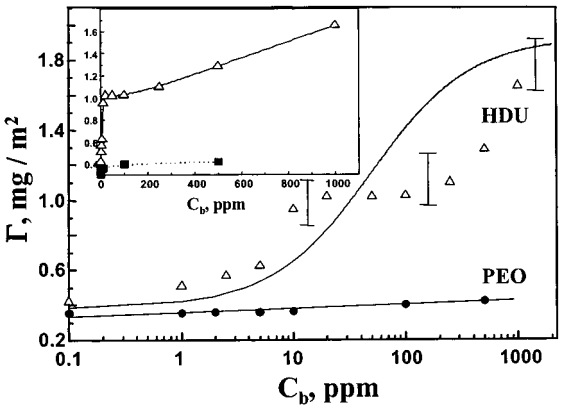

Figure 3. Adsorption isotherms of PEO and HDU, on silica. Data for 33 K PEO adsorption were taken from ref 31. The line through the PEO data is an isotherm motivated by mean field theory, per eq 3. The curve through the HDU data follows eq 4, where c_o is chosen to be 10 ppm, and Γ_o and L follow with values of 0.4 and 1.5 mg/m^2, respectively. p becomes 0.00898 mg/m^2 ppm and then a fit for K yields 0.02 ppm^{-1}.

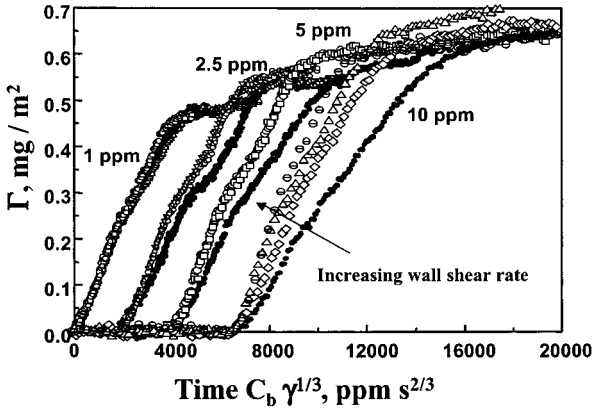

Figure 4. Adsorption runs at different concentrations and wall shear rates. Each group of data for a particular concentration has been arbitrarily shifted for ease of viewing. For each concentration, runs with wall shear rates of 1, 5, and 27 s^{-1} are presented. At 10 ppm, there is an additional run with a wall shear rate of 8.5 s^{-1}.

we cannot currently distinguish whether these associated hydrophobes are in contact with the silica or merely in the interphase.

To further probe the feasibility of the proposed interfacial structure, Figure 3 compares the adsorption isotherm of HDU with that of PEO, where data for the latter were taken from ref 31. The logarithmic scale facilitates a close examination of the dilute solution regime and is appropriate for polymer adsorption, while the standard representation with the linear concentration axis is shown in the inset. For the unmodified PEO, the coverage is relatively independent of free solution concentration over many decades of concentration, as expected for homopolymers adsorbing in the classical layer structure of loops, tails, and trains.[35] In contrast, the coverage of HDU is concentration-dependent. In the dilute limit, the HDU coverage approaches that of PEO, while above about 5 ppm, the HDU coverage increases with concentration. The convergence of the two isotherms in the dilute limit suggests that an underlying HDU layer is indeed similar to the classical unmodified PEO layer.

The HDU data between 10 and 100 ppm seem to indicate a pseudoplateau; however, we interpret this feature with caution: The slow approach to the ultimate HDU coverages contributes to experimental error in isotherm measurement, since experiments longer than a few hours are subject to signal drift. At the highest concentrations, the coverage continues to increase, consistent with network formation in concentrated solutions. It will be discussed in detail later that, above about 10 ppm, the coverage exhibits a mild dependence on wall shear rate. These isotherms were measured at relatively gentle wall shear rates which, for the high polymer concentrations, gave the greatest adsorbed amounts.

In the inset of Figure 3, the linear concentration axis representation masks the fact (made apparent on the logarithmic scale) that there is an underlying HDU population that is strongly physisorbed and whose limiting dilute coverage is similar to that of homopolymer PEO adsorbing by its main backbone. Examining only the linear concentration representation might lead one to erroneously conclude that the rounded HDU isotherm shape extends down to the dilute regime and that a weak Langmuir adsorption constant applies to all chains within the layer.[9,23] In the final section of the results and discussion, we explore in detail the implications of isotherm shape on desorption kinetics. In Figure 3, the lines represent fits to isotherm models that are developed in that context.

Adsorption Mechanism: Chains or Clusters? One interesting issue concerning the adsorption of the polymers in the current work, or the adsorption of micelle-forming polymers in general, is the extent to which single chains versus micelles or associated clusters adsorb. The initial adsorption kinetics, for instance, those in Figure 4, provide some insight into this question. Figure 4 plots the evolving coverage on the y-axis as a function of normalized time on the x-axis.

For each adsorption run, of which there are many in Figure 4, buffer initially flows through the cell. A valve is turned over and HDU solution flows through the cell, initiating adsorption at time zero. In Figure 4, the various runs have been conducted at different wall shear rates and bulk solution concentrations. The time axis has been multiplied by bulk solution concentration (C_b) and by wall shear rate (γ) to the 1/3 power, which tends to collapse runs to a master curve. The runs are clustered in groups, each representing a particular concentration. The wall shear rate is varied within each group. Data for the different concentrations are separated horizontally by an arbitrary shift along the horizontal (time) axis to facilitate viewing.

The normalization of the x-axis in Figure 4 is motivated by the Leveque solution to the convection−diffusion equation for transport-limited adsorption in a slit shear cell such as ours:

$$\frac{d\Gamma}{dt} = 0.538\left(\frac{\gamma}{L}\right)^{1/3} D^{2/3}\, C \qquad (1)$$

Here, L is the distance from the cell entry to the point of observation, and D is the free solution diffusivity of the adsorbing species. The form in eq 1 has been discussed extensively by us[31] and by others.[37,38] It holds when a pseudo-steady state is established, for instance, when the adsorption process is sufficiently long that the concentration gradient near the interface is constant for most of the

(35) Scheutjens, J. M. H. M.; Fleer, G. J. *J. Phys. Chem.* **1979**, *83*, 1619−1635.

(36) Leveque, M. A. *Ann. Mines* **1928**, *13*, 284.

(37) Lok, B.; Cheng, Y.-L.; Robertson, C. R. *J. Colloid Interface Sci.* **1983**, *91*, 104.

(38) Shibata, C.; Lenhoff, A. *J. Colloid Interface Sci.* **1992**, *148*, 485.

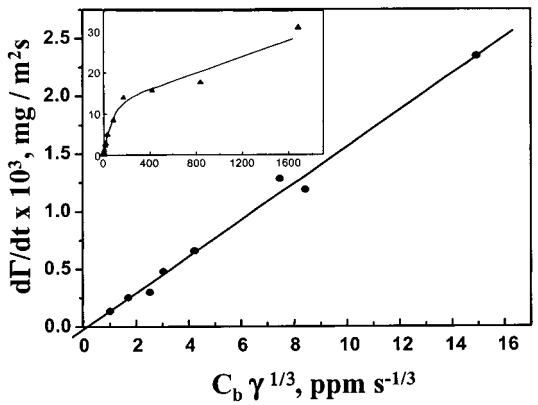

Figure 5. Adsorption rate as a function of free solution concentration and wall shear rate, as a means of testing eq 1. Data in the main figure include free solution concentrations up to 5 ppm, while concentrations in the inset go up to 1000 ppm.

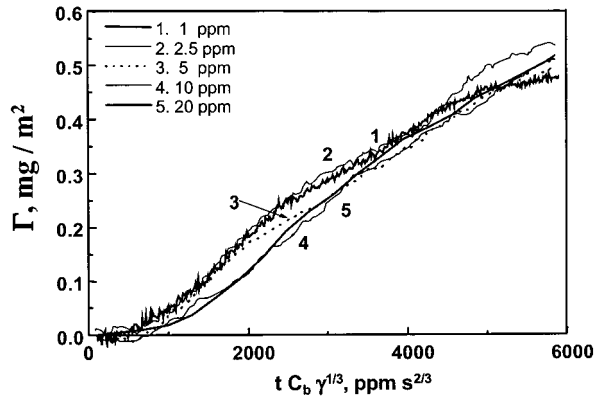

Figure 6. Collapsing adsorption runs for different free solution concentrations and a wall shear rate of 5 s^{-1}.

adsorption process. This has been shown to hold for PEO adsorption on silica when the bulk solution concentration is 15 ppm or less for molecular weights of 30−50 K.[31] To the extent that adsorption is transport-limited, eq 1 would also be expected to apply for HDU adsorption.

In Figure 4, the collapse of the data from 1 to 5 ppm, at all but the lowest wall shear rate of 1 s^{-1}, indicates transport-limited adsorption per eq 1. For the conditions where the data do collapse, the initial slopes are consistent not only with the 1/3-power law dependence on wall shear rate but also with the direct proportionality with concentration, as summarized in the main part of Figure 5. The curvature in the inset of Figure 5, representing apparent deviation from the Leveque form, sets in at bulk solution concentrations near 10 ppm, where the curves in Figure 4 are spread. Also in the inset, the bulk solution concentrations go up to 1000 ppm. At high concentrations, deviation from eq 1 is substantial because of breakdown of the pseudo-steady-state approximation. From 1 to 10 ppm at the lowest wall shear rate, deviation from eq 1 stems from origins other than the breakdown of the pseudo-steady-state approximation, as will be discussed below. Figure 6 emphasizes the influence of concentration at the modest wall shear rate of about 5 s^{-1}. Here again, adsorption traces for the most dilute solutions collapse exactly.

In Figure 4 at 10 ppm or at 5 ppm under the conditions of the gentlest shear, the data do not collapse to a master curve. Especially at 10 ppm, the shear rate effect is no longer consistent with eq 1, even though the Leveque form should still hold, since there is sufficient time for a pseudo-steady-state concentration gradient to develop, per ref 37. The breakdown of the superposition must be from other origins. We propose and will provide evidence for the hypothesis that, at high concentrations, polymer clusters or aggregates contribute significantly to the initial adsorption kinetics, while in the dilute limit, only single chains, or dimers at most, adsorb. Further, the size of the adsorbing clusters appears to depend on the wall shear rate.

In Figure 4, the adsorption traces for HDU had the unusual feature of a slight shoulder near 0.3−0.35 mg/m^2, prior to the ultimate coverage of 0.5 mg/m^2 or more. Also, after the initial surface saturation, the coverage slowly increased as long as the polymer solution continued to flow. The slow increase and the shoulder were both highly reproducible, and both features were preserved in the master curves resulting from normalization on wall shear rate. The ultimate slow increase in coverage at these dilute concentrations can be explained by slight sample polydispersity, similar to the arguments put forth for unmodified PEO.[26−29] In the dilute regime of Figure 4, most of the HDU chains are adsorbed to the silica, and polydispersity causes long chains to displace short ones during continued polymer flow, increasing the interfacial mass. We focus our attention away from this artifact in the current work. (The isotherm coverages in Figure 3 are those from the primary saturation shoulder, avoiding the polydispersity artifact.)

The shoulder at about 0.3−0.35 mg/m^2 is highly reproducible and is most pronounced in the dilute limit. Beyond this shoulder, the adsorption is *slightly* slower. The coverage at the shoulder is significant in that 0.35 mg/m^2 corresponds to the saturation coverage of unmodified PEO. The adsorption rate prior to the shoulder corresponds to the transport-limited adsorption of single chains. The slower adsorption rate after the shoulder may correspond to the adsorption of additional chains by hydrophobic association. Since the affinity for the more loosely bound chains is weaker than for the underlayer, a finite free solution concentration must exist in the fluid nearest the surface, per the isotherm in Figure 3. This provides a smaller driving force for the diffusive flux of chains to the interface and therefore a slightly slower rate of adsorption once the underlayer is established.

At concentrations of 10 and 20 ppm, the initial adsorption rate is slightly slower, on a normalized time axis, than the adsorption rate in the most dilute solutions, in Figure 6. This suggests that the diffusion coefficient of the adsorbing species is smaller at the higher concentrations, perhaps as a result of cluster formation.

Returning to Figure 4, at 10 ppm the adsorption traces at various wall shear rates do not collapse when the time axis is scaled on $\gamma^{1/3}$. One explanation is that the diffusivity of the adsorbing species changes with wall shear rate, in eq 1. This would imply different hydrodynamic radii of the adsorbing species at different wall shear rates, or that the flow, as gentle as it is, can break the associative clusters. A second explanation would be that the fundamental adsorption rate is affected by the wall shear rate. This latter idea becomes less appealing when one notes, in Figure 4, that the normalized adsorption rate is affected by the wall shear rates even at the shortest times when the coverage is lowest. If one believes that the underlayer adsorbs through hydrogen bonding of the surface, one would not expect this hydrogen bonding adsorption mechanism to be slower than the transport-limited rate. Studies with native PEO in this range of concentrations and wall shear rates have shown transport-limited behavior, that is, normalization of the adsorption rate on $\gamma^{1/3}$ removes any further dependence on wall shear rate.[31]

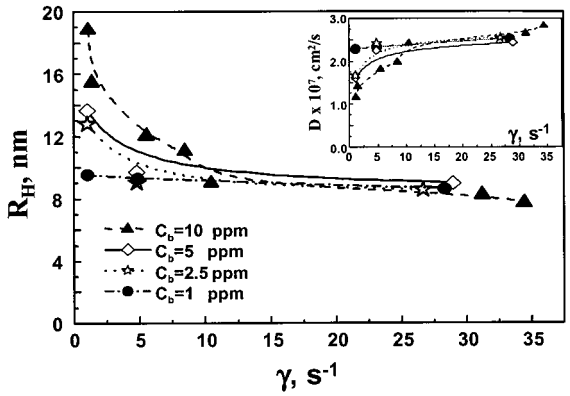

Figure 7. Diffusivity and hydrodynamic size of the dominant adsorbing species.

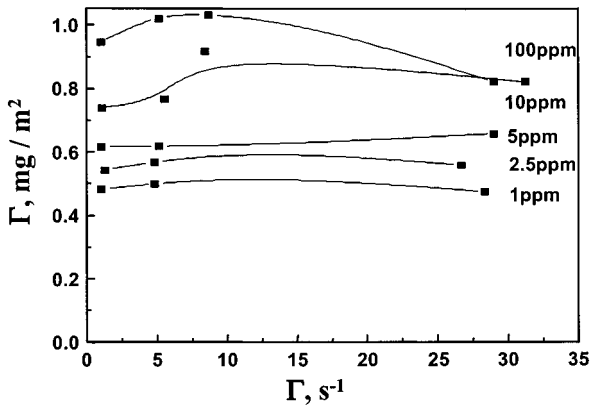

Figure 8. Influence of wall shear rate on the ultimate HDU surface coverage, for different free solution concentrations.

Figure 7 explores the apparent diffusivity (obtained from application of eq 1 to the data in Figure 4) and hydrodynamic radius, R_H (obtained from the diffusivity through the Stokes Einstein equation), of the adsorbing species as a function of concentration and wall shear rate. In the dilute limit, the adsorbing species has a diffusivity of about 2.7×10^{-7} cm^2/s and a hydrodynamic radius of about 8−9 nm. This is slightly slow, or large for unmodified PEO of molecular weight 32.6 K, where we previously reported a coil size of 6.2 nm.[31] The dilute-limiting diffusivities in the current work are, however, in reasonable agreement with pulse gradient NMR measurements of a 34 K sample of unmodified PEO, where $D = 3.1 \times 10^{-7}$ cm^2/s and $R_H = 7.9$ nm.[15,17]

In Figure 7, larger adsorbing entities, clusters, are found at concentrations of 10 ppm. In the limit of zero shear, a diffusivity of $1.2-1.3 \times 10^{-7}$ cm^2/s and a hydrodynamic radius of 17 ± 1.5 nm is found. These results are in excellent agreement with the light-scattering data of Pham et al. who report associated micelles of 17 ± 0.4 nm with this HDU sample, albeit at a higher concentration of 200 ppm.[5] These clusters correspond to an aggregation number of 20 chains/micelle. Pham et al. did not explore the dilute regime studied in the current investigation, and we were unable to quantify cluster sizes at greater concentrations because of the breakdown of the pseudo-steady-state approximation leading to eq 1, at concentrations exceeding 20 ppm. Fluorescence studies revealed in the dilute limit, aggregation number, and therefore micelle size, should be insensitive to concentration.[14,15] Our data therefore suggest that significant amounts of micelles persist at concentrations as low as 10 ppm, but single chains dominate at 1 ppm. These clusters are, however, apparently very fragile as they give way to single chains at wall shear rates of 10 s^{-1}.

It is extremely interesting that we begin to see the formation of micelles in solution near 10 ppm. This bulk solution concentration for micellization also corresponds to the build up of interfacial mass via hydrophobic associations, in the isotherm of Figure 3. Below this micellization concentration of 10 ppm, the adsorbed HDU layer is similar to that of unmodified PEO, consisting of chains hydrogen bonded directly to the silica with coverages near 0.4 mg/m^2.

Breaking Interfacial Associations. The adsorption/desorption dynamics, adsorption isotherm shape, and crossover in adsorption kinetics from single chain to micelle adhesion all point to a model where adsorbed layers of associative polymers contain an underlayer dominated by attractions between the main backbone and the substrate and where a more tenuous outer region is dominated by hydrophobic associations. This hydrophobically associated outer layer was found to impart a mild shear dependence on the total ultimate coverage, shown in Figure 8. We find the highest coverages at the lowest wall shear rates; though, in the gentle regime, there is a slight maximum which is not yet explained. At wall shear rates of 30 s^{-1}, the total ultimate coverage decreases when the free solution concentration is 10 ppm or greater. For layers adsorbed from more dilute solutions, shear has no significant effect on the ultimate coverage because at these more dilute concentrations there is no loosely bound layer. The layers are primarily adsorbed via hydrogen bonds between the main backbone and the substrate in the dilute regime. This is similar to the adsorption of unmodified PEO, which also does not exhibit a wall shear rate dependence on coverage.[31] In future studies, we plan to more completely investigate the influence of wall shear rate on coverage. In the current investigation, we have included the maximum flow rates available with the current equipment.

The data in Figure 8 suggest that chains, adsorbed in the interphase through hydrophobic associations, set up a hydrodynamically influenced equilibrium that determines the ultimate coverages. A closer examination of the desorption dynamics provides further insight to the role of hydrophobic associations.

In developing our ideas about desorption dynamics and hydrophobic associations, we start from the perspective of the desorption kinetics of PEO layers from silica in aqueous solution, which is exceedingly slow and has been quantified by Dijt and co-workers.[32] The critical underlying concept is that in many cases, desorption kinetics can be mass-transport limited, in a fashion similar to the transport-limited adsorption kinetics that abound in polymer adsorption. In such cases, local equilibrium is maintained between an adsorbed layer and fluid nearest the interface. The desorption kinetics is then limited by the flux, J, of chains away from the interface, according to a mass-transfer coefficient, M, which is well quantified for flow systems such as ours:

$$d\Gamma/dt = J = M\,(C_b - C^*) \qquad (2a)$$

Here, C_b is the bulk solution concentration of polymer while C^* is its local concentration in the fluid nearest the adsorbed layer. The mass transfer coefficient M derives from eq 1, according to

$$M = 0.538\left(\frac{\gamma}{L}\right)^{1/3} D^{2/3} \qquad (2b)$$

During desorption, C_b is maintained to be zero by continuous flow of solvent over the layer; however, locally in the boundary layer, the free polymer concentration may not be zero, maintaining C^* at some finite but very small value.

For classical homopolymer layers of tails, loops, and trains, the coverage is only weakly dependent on free solution concentration, as shown in Figure 3, and is also predicted from self-consistent mean field theory.[35] This motivates the following form for an isotherm of unmodified PEO (used by Dijt et al.):[32]

$$\Gamma(c) = \Gamma_o + p \log(c/c_o) \qquad (3)$$

Equation 3 is simply a line on a semilog isotherm plot, per Figure 3. Γ_o is the coverage measured at some arbitrarily chosen concentration, c_o, needed to fix an intercept on the logarithmic x-scale. p is the slope of the isotherm, which for unmodified PEO was found to be 0.008981 mg/m^2 ppm in Figure 3, giving the linear isotherm fit. Dijt and coworkers combined eqs 2 and 3, setting $C_b = 0$, to predict the desorption kinetics and showed reasonable agreement with PEO desorption.[32] This demonstrated that PEO desorption, though exceedingly slow, was still transport-limited. Even slower desorption would need to be observed if one wanted to invoke explanations involving more complicated physics such as interfacial glasses or a finite interfacial desorption rate constants. The rate observed, corresponding to the transport limit, was the fastest possible.

With our ultimate goal of relating the hydrophobe physics to the interfacial network dynamics, that is, the desorption of the hydrophobically associated outerlayer, it was first necessary to consider whether the desorption of the loosely bound layer was transport-controlled. Since transport-limited desorption involves local equilibrium in the boundary layer, we hypothesized a form for the adsorption isotherm of HDU:

$$\Gamma(c) = L \frac{Kc}{1 + Kc} + \Gamma_o + p[\log(c) - \log(c_o)] \qquad (4)$$

This isotherm is a hybrid of the Langmuir form, with binding constant K which applies to the loosely bound chains, and the linear form in eq 3, which applies to the tightly bound underlayer. The constants L and Γ_o describe the relative amounts loosely bound chains and those which are hydrogen bonded to the surface directly. Equation 4 fits the HDU isotherm data in Figure 3 reasonably well, with c_o = 10 ppm, Γ_o = 0.4 mg/m^2, L = 1.5 mg/m^2, p = 0.00898 mg/m^2 ppm, and K = 0.02 ppm^{-1}.

To predict the desorption dynamics, eqs 4 and 2 were combined, setting $C_b = 0$ and using c^* for the concentration in eq 4. This led to

$$t = \int_{\Gamma_{init}}^{\Gamma(t)} \frac{d\Gamma}{-Mc^*(\Gamma)} \qquad (5)$$

which was solved numerically. Here, $c^*(\Gamma)$ is the inversion of the isotherm function in eq 4. That is, instead of coverage as a function of free concentration, we use free concentration as a function of coverage.

To test eq 5, we conducted a series of studies in which sets of adsorbed layers, all deposited and aged at identical conditions of wall shear rate and bulk solution concentrations, were subject to different wall shear rates during desorption. Figure 9 shows an example of the desorption traces on a log scale. The inset illustrates the three runs on a linear scale, showing the high reproducibility of the initial adsorption traces. The fits to the desorption traces all have identical values for K, L, Γ_o, and p. Only the mass transfer coefficient varied per eq 2b, as the wall shear rate was changed for the desorption portion of the three traces.

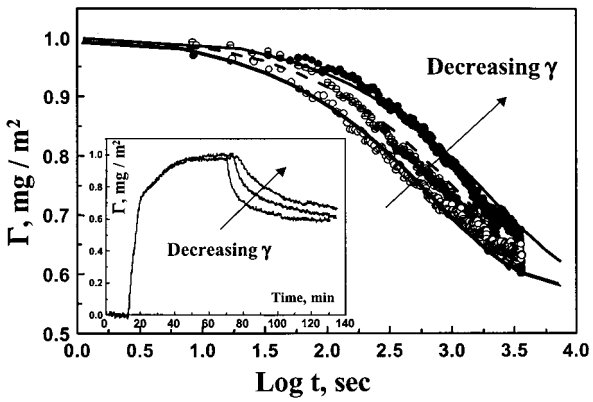

Figure 9. Desorption data, with full adsorption shown in the inset, for a bulk solution concentration of 10 ppm and three different wall shear rates: 1.1, 5.1, and 29 s^{-1}. The lines are fits to the three runs with L = 0.4 mg/m^2, p = 0.0898 mg/m^2 ppm, $D = 2.7 \times 10{-}7$ cm^2 s^{-1}, and K chosen to be 0.002 ppm^{-1}.

There is excellent agreement between eq 5 and the data. Though it may first appear that there are many parameters which could be chosen to accomplish this fit, most of these are eliminated independently, for instance, the p value which was based on the isotherm of unmodified PEO. The values of L = 0.4 mg/m^2 and Γ_o = 0.6 mg/m^2 are within reason and were chosen to be identical for all three runs. The primary fitting parameter, K = 0.002 ppm^{-1}, was fit once for all three runs. With these equilibrium parameters fixed, the spread in the three data sets follows exactly from the mass transfer coefficients, which derive from eq 1 and depend on wall shear rate which was controlled experimentally. (We employed a diffusivity of 2.7×10^{-7} cm^2/s for single chains, since bulk rheological measurements suggest control by disengagement of single hydrophobes from associated junctions.)

The fit of eq 5 to the desorption data strongly suggests that the observed dynamics are indeed transport-limited. It is no coincidence that the variations in M exactly predict the horizontal shifts in the data sets. Local equilibrium is maintained between the hydrophobically associated chains and those nearby in the boundary layer. The next issue, then, is the extent to which the isotherm model is physically meaningful. Both the dynamics and equilibrium suggest that consideration of two interfacial populations may be a very reasonable first approximation of the energetics.

The K value of 0.002 ppm^{-1} is in excellent agreement with that reported by Pham et al.[23] for adsorption of ODU (having octadecyl rather than hexadecyl end-group hydrophobes, but otherwise very similar to our HDU) onto PMMA latex. Our K value corresponds to an adsorption energy of 7.6 kT/chain,[39] which is similar to Pham's result of 7 kT and well within the range of 5−13 kT reported by a variety of laboratories[9,23] for related systems. However, these other groups reporting Langmuir binding constants did so by fitting the Langmuir form to their data, using a linear concentration axis and employing all the data in

(39) Conversion of the equilibrium constant to an adsorption free energy, ΔG, requires a definition of a fractional coverage. We choose the convention employed by refs 23 and 9, which implies comparison to the maximum coverage. Since the maximum coverage depends on a balance between free energy and excluded volume, ΔG is ill-defined but meaningful in a comparative sense.

their fit. In most instances, their range of concentrations included conditions more concentrated than ours. For this reason, their fitting processes tended to neglect any tightly bound chains at low coverages.

While we report similar "adsorption energies" to the other groups, we emphasize that our value corresponds to the hydrophobic association energy of the loosely bound chains that participate in interfacial clusters. Our K value and adsorption energies do not correspond to the tightly bound underlayer and do not describe polymer−surface interactions which can be as high as 50−100kT/chain.[35] The latter are captured by p and Γ_o in eq 4. We believe that, in many of these other laboratories, tightly bound underlayers may have been present but could not be resolved because of the experimental error of particular isotherm measurement techniques. (This is the case, especially for isotherms where the free solution concentration on the x-axis was determined by chemical or refractive index assay.) The K values and adsorption energies reported by the other labs were most likely dominated by the loosely bound chains but attributed more generally to polymer−surface interactions. The current work specifically attributes the modest adsorption energies from the K values to the loosely bound population.

Both desorption and isotherm experiments contain information about the shape of the adsorption isotherm. When desorption can be proven to be transport-limited, the isotherm information can be obtained with less uncertainty than direct isotherm measurements. Better yet, a single desorption experiment, starting with a layer that was adsorbed from a relatively high free solution concentration can, in theory, probe the entire adsorption isotherm. Generating an isotherm via the classical method requires independent measurement of many data points and is more time-consuming. Additionally, point-by-point measurement of an isotherm is subject to polydispersity artifacts and other experimental complications. Desorption data probe the isotherm more precisely. Point-by-point adsorption data are, however, most effective in the extremely dilute regime, which may be difficult to access via the desorption procedure.

With this said, we can now comment on the differences in the K values obtained from the desorption traces in Figure 9 and the direct isotherm fit in Figure 3. In the regime above 10 ppm in Figure 3, the coverage increases with concentration, as does the uncertainty. Our investigation did not explore free concentrations above 1000 ppm; however, at our highest concentrations, the coverage is increasing sharply. Because we have not reached the plateau of the isotherm, we cannot accurately identify the inflection point in the Langmuir portion of the fit. In other words, we have not yet reached the onset of the isotherm plateau, which is critical in estimating K. This also explains the discrepancy in L values between the fits in Figures 3 and 9. The K values from the direct fit to the isotherm in Figure 3 appear large (i.e., shifted left) compared with what we know from the literature,[23] and more importantly, from the desorption experiments in Figure 9.

Conclusions

This work examined the adsorption isotherm and the adsorption and desorption kinetics of a model associative polymer, in the limit of strong interactions between the substrate (in this case silica) and the polymer's main backbone. Both dynamic and static experiments support a scenario where the layer is comprised of two main populations: a tightly bound underlayer driven primarily by substrate-PEO interactions and a hydrophobically associated outer layer which is shear-responsive. The adsorbed mass of the tightly bound underlayer is similar, in the dilute limit, to that of native PEO on silica, suggesting that the underlayer's structure is comprised of tails, loops, and trains similar to layers of classically adsorbed homopolymers. The chain ends in the tightly adsorbed underlay may, however, participate in interfacial clusters. The loosely bound outer layer is present at concentrations greater than modest dilution, above about 10 ppm.

The adsorption kinetics and the shape of the adsorption isotherm are correlated. In the dilute limit, well below 10 ppm, single chains adsorb at the transport-limited rate, controlled by their free solution hydrodynamic radii. At these conditions, the surface saturates once the tightly bound underlayer is in place, with minimal amounts of hydrophobically associated chains at the interface. At more concentrated conditions, whole micelles adsorb at a transport-limited rate dictated by their larger free solution hydrodynamic radius. In this regime, the surface saturates after both the tightly bound underlayer and loosely bound layer are in place. The hydrodynamic sizes of the individual chains and the associated clusters, or micelles, are consistent with findings of other groups for the same materials.

The loosely bound outer layer exhibits an interesting dependence on wall shear rate. First, the steady-state coverage goes through a maximum and ultimately decreases with increased shear rate, behavior reminiscent of the slight shear thickening and substantial ultimate shear thinning in concentrated solutions. Second, the loosely bound layer is gradually removed by continuous flow of buffer solution without free polymer. The chains are washed from the interface and hydrophobes escape junctions at the transport-limited rate, maintaining local equilibrium between the loosely bound layer and chains in the nearby fluid.

While the two-population concept is a simplification, with a broader distribution existing at real interfaces, a simple quantitative model sufficiently captures the adsorption physics. We treat the adsorbed layer as a hybridization of the classical homopolymer isotherm shape (from mean field theory) and a Langmuir form for the hydrophobically associated chains. This approach qualitatively predicts the shape of the isotherm and, when combined with expressions describing mass transport between the bulk solution and the interface, quantitatively predicts desorption kinetics. From the desorption kinetics, the strength of the hydrophobic junctions can be estimated and was found to lie between 7 and 8 kT, in excellent agreement with "sticking energies" reported by other laboratories.

Acknowledgment. This work was made possible by NSF through grant CTS-9817048. HDU samples were generously donated by Dr. W. Lau of the Rohm and Haas Company.

LA0111912